Journal of Applied Research in Water and Wastewater
E-ISSN: 2476-6283
Journal homepage: https://arww.razi.ac.ir

Assessing and mitigating the thermodynamic biases of satellite precipitation products in a water-scarce environment

Mahdi Naseri*, Mitra Noorizehab

Department of Civil Engineering, Faculty of Engineering, University of Birjand, Birjand, Iran.

GRAPHICAL ABSTRACT

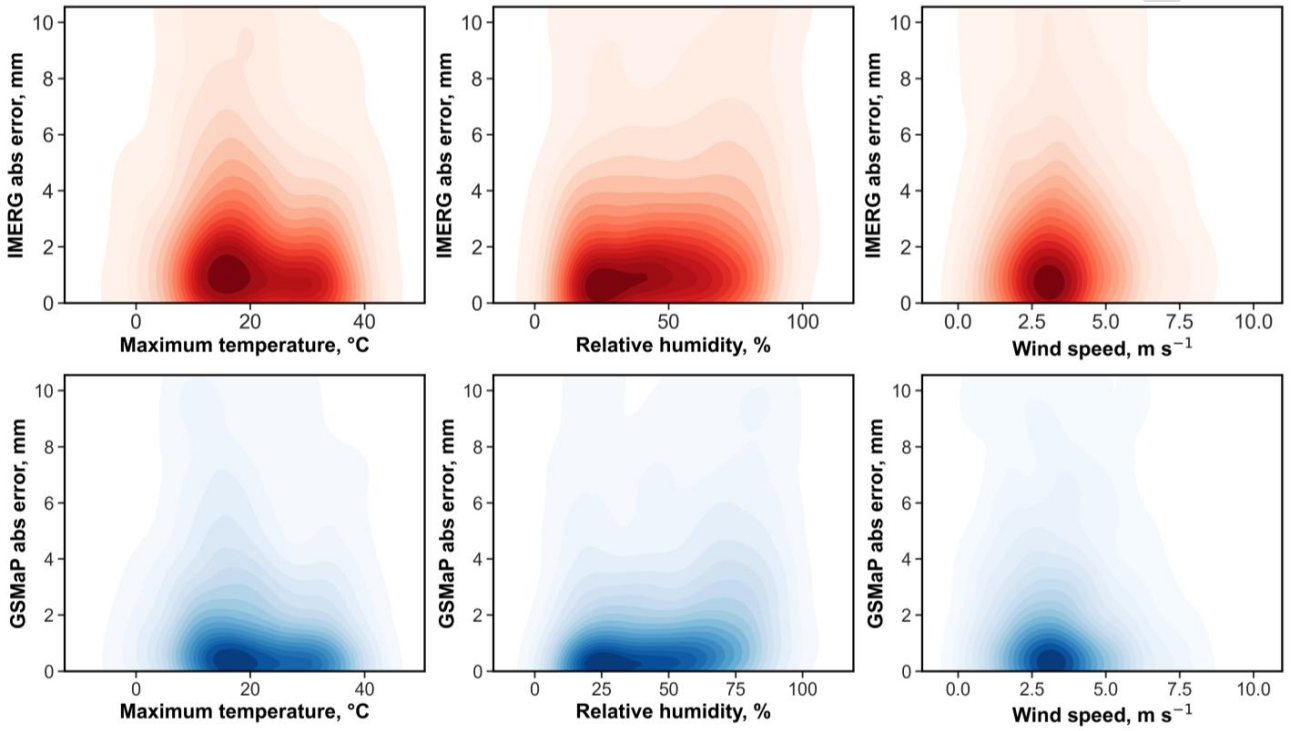

ARTICLE INFO

Article type:
Research Article

Article history:
Received xx Month xxx
Received in revised form xx Month xxx
Accepted xx Month xxx
Available online x Month xx

Keywords:
Satellite precipitation products
Error evaluation
Multiple linear regression
Hyper-arid climate

ABSTRACT

Accurate precipitation estimation in hyper-arid regions is fundamentally challenged by sparse observational networks and complex atmospheric dynamics. This study evaluates and corrects the errors of IMERG (Final V07) and GSMaP satellite precipitation products using 18 years (2005–2023) of daily synoptic data from Birjand, representing the hyper-arid climate of eastern Iran. Baseline evaluations indicated that GSMaP outperformed IMERG in continuous metrics (RMSE = 3.25 vs. 4.40 mm/day); however, both exhibited systematic underestimation, primarily driven by sub-cloud evaporation (the Virga effect). Categorically, IMERG demonstrated higher detection sensitivity (POD = 0.763), whereas GSMaP more effectively minimized false alarms. Bivariate density analysis revealed a notable finding: absolute estimation errors are significantly driven by surface thermodynamic conditions (maximum temperature and relative humidity, P-value < 0.01), while the dynamic impact of wind speed was statistically insignificant. Finally, applying a multiple linear regression (MLR) bias correction framework incorporating these meteorological covariates successfully reduced IMERG's RMSE by 14.1%. The findings demonstrate that integrating surface thermodynamic data with satellite retrieval algorithms via regression models substantially mitigates precipitation uncertainties in data-scarce hyper-arid basins.

1. Introduction

Precipitation is a fundamental component of the global hydrological cycle, playing a critical role in water resource management, climate modeling, flood forecasting, and drought monitoring (Cao *et al.* 2025; Conte *et al.* 2026). Access to continuous and accurate precipitation data is particularly vital in arid and semi-arid regions, which are highly vulnerable to extreme spatial and temporal rainfall variability and severe water scarcity (Li *et al.* 2025) and severe water scarcity, which frequently exacerbate the functional challenges of groundwater management and aquifer recharge in these plains (Akbarpour *et al.* 2024; Shamshirgaran *et al.* 2025). Traditionally, ground-based rain

*Corresponding author Email: mnaseri@birjand.ac.ir

Cite this article: M. Naseri, M. Noorizehab, Assessing and mitigating the thermodynamic biases of satellite precipitation products in a water-scarce environment, *Journal of Applied Research in Water and Wastewater*, x (x), 202x, xx-xx. doi: https://doi.org/10.22126/arww.2026.13707.1480

gauge networks have been considered the most reliable source of precipitation measurements (Zhang *et al.* 2025b). However, their sparse distribution, high maintenance costs in remote or rugged terrains, and susceptibility to measurement errors caused by wind and evaporation significantly limit their large-scale applicability (Saeed Abdelrazaq *et al.* 2026; Mardani *et al.* 2025).

To overcome these limitations, satellite precipitation products (SPPs) have emerged as an effective alternative, offering extensive spatial coverage and high temporal resolution (Pellicone *et al.* 2025; Tosan *et al.* 2024). Following the launch of the global precipitation measurement (GPM) mission, a new generation of high-resolution products such as the Integrated Multi-satellitE Retrievals for GPM (IMERG) and the global satellite mapping of precipitation (GSMaP) was introduced (Meng *et al.* 2025). By integrating observations from passive microwave (PMW) and infrared (IR) sensors, these products have substantially improved global precipitation estimation (Ji *et al.* 2025). Despite these technological advancements, satellite retrievals still exhibit systematic biases and uncertainties rooted in sensor limitations, retrieval algorithm assumptions, and complex topographic interactions (Gou *et al.* 2026; Tosan *et al.* 2026a). In hyper-arid climates, a major challenge is the sub-cloud evaporation phenomenon, commonly known as Virga, where falling raindrops evaporate before reaching the surface (Baig *et al.* 2025). Satellite sensors often misclassify these signals as surface precipitation, leading to significant overestimation and false alarms (Shirmohammadi Aliakbarkhani *et al.* 2025).

Recent studies emphasize that the performance and error margins of satellite products are strongly modulated by local thermodynamic and dynamic atmospheric conditions (Xiong *et al.* 2025; Montiel *et al.* 2026). Meteorological variables such as air temperature, relative humidity, and wind speed can alter the signals received by sensors and affect the detection of the precipitation phase (Bisht *et al.* 2025). Therefore, a purely statistical evaluation of these products is insufficient; exploring the physical relationships between satellite errors and meteorological variables is crucial. Consequently, applying machine learning and regression-based bias correction frameworks that incorporate auxiliary meteorological variables has been proposed as a novel approach to enhance the accuracy of satellite data in ungauged or sparsely gauged regions (Yao *et al.* 2024).

Despite numerous global evaluations of GPM-era products, their behavior under the specific hyper-arid climatic conditions of eastern Iran, as well as the identification of meteorological drivers affecting their errors, remains insufficiently explored. A critical synthesis of recent literature (2025–2026) reveals that while numerous studies have evaluated GPM-era products across various topographies, the majority have treated satellite biases as purely statistical phenomena to be corrected via mathematical mapping (e.g., Baig *et al.* 2025; Xiong *et al.* 2025). Although some recent investigations have acknowledged the influence of meteorological parameters on retrieval accuracy (Bisht *et al.* 2025), a clear methodological gap remains: the physical mechanisms driving these errors, specifically the thermodynamic sub-cloud evaporation (Virga effect) in hyper-arid environments, are rarely integrated directly into the bias correction algorithms as dynamic physical constraints. Existing literature often relies on complex, black-box machine learning models that, while statistically robust, lack physical interpretability regarding how atmospheric temperature and humidity independently force satellite overestimations in water-scarce regimes, a fundamental challenge recently highlighted in the push for Explainable AI (XAI) and advanced multi-source data fusion (Nourani *et al.* 2025; Tosan *et al.* 2026b).While previous studies have extensively evaluated satellite precipitation products using standard statistical metrics, few have deeply investigated the physical and thermodynamic drivers of these errors in hyper-arid environments. The main novelty and scientific contribution of this study lie in transitioning from a purely descriptive statistical evaluation to a physically-driven framework. By decoding the meteorological factors (i.e., temperature, humidity, and wind speed) influencing IMERG and GSMaP uncertainties and consequently proposing a thermodynamic-based MLR model, this work provides a practical and lightweight approach to mitigate systematic biases in data-scarce regions.

To address this gap, this study provides a comprehensive evaluation and bias correction of IMERG and GSMaP precipitation products using long-term synoptic data from the Birjand station, representing the hyper-arid climate of eastern Iran. The specific objectives of this study are to: 1) conduct a baseline continuous and categorical evaluation of satellite products against ground observations; 2) analyze the sensitivity of satellite absolute errors to thermodynamic and dynamic atmospheric variables (temperature, humidity, and wind speed) using bivariate density distributions; and 3) develop a bias correction framework based on multiple linear regression (MLR) to mitigate uncertainties and provide reliable climate data for sustainable water resource management in the region.

2. Materials and methods

2.1. Study area and datasets

This study focuses on Birjand, the capital city of South Khorasan province in eastern Iran, geographically situated at approximately 32°52' N latitude and 59°12' E longitude (Fig. 1). Based on the De Martonne and Ivanov climate classification indices, the region is characterized by a hyper-arid and desert climate (Tosan and Maroosi, 2024). The mean annual minimum and maximum temperatures in Birjand are 8 °C and 24 °C, respectively. The area experiences a substantial mean annual potential evapotranspiration of approximately 2,700 mm against a sparse and highly variable average annual precipitation of only 120 mm (Ramezani Moghadam *et al.* 2018). This limited rainfall is primarily driven by Mediterranean synoptic systems during the winter months and sporadic convective showers in the spring. The limited and highly variable water resources in this region are exceptionally critical for sustaining high-value agricultural crops, particularly saffron, whose yield and production challenges are strictly tied to hydro-climatic fluctuations (Feizi and Tosan, 2017; Rezvani Moghaddam *et al.* 2016; Yaqubi *et al.* 2024).

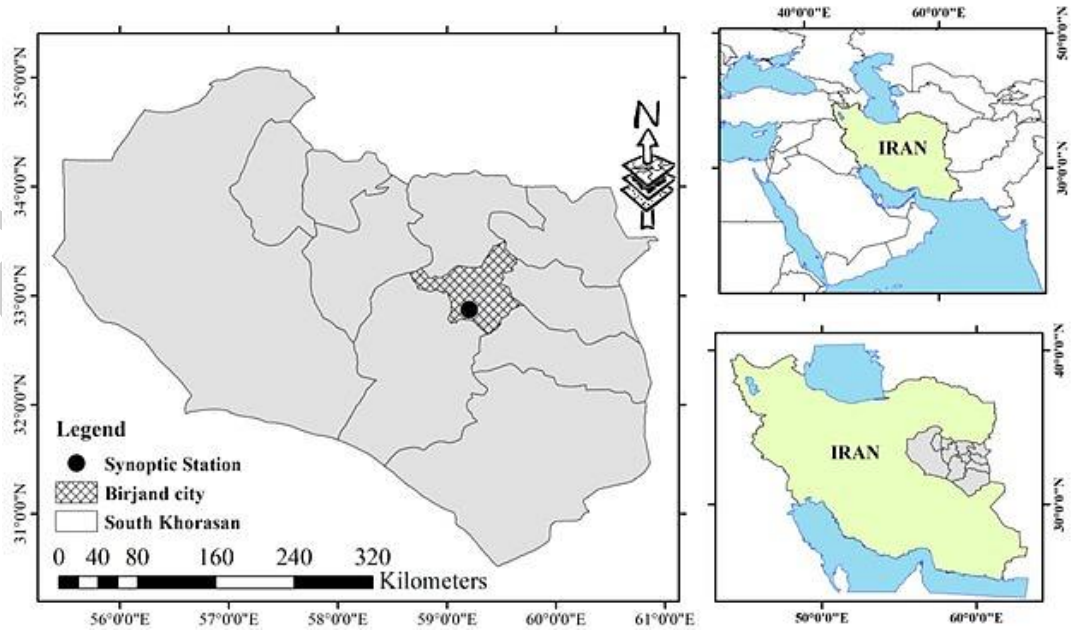

Fig. 1. Location map of the study area and Birjand Station.

The reference dataset comprises daily ground-based meteorological observations obtained from the Birjand synoptic station for a long-term period from 2005 to 2023. The extracted variables include daily precipitation (Pobs), maximum temperature (Tmax), relative humidity (RH), and wind speed (WS). For the satellite precipitation datasets, two state-of-the-art products were utilized: the IMERG Final Run (V07) and the GSMaP product. Both products offer a high spatial resolution of 0.1° × 0.1° and were aggregated to a daily temporal scale to match the ground observations over the identical 18-year period.

2.2. Statistical evaluation metrics

To benchmark the accuracy of the satellite products against the ground observations, a suite of widely adopted continuous statistical metrics was employed. These metrics include the Pearson correlation coefficient (CC), root mean square error (RMSE), mean absolute error (MAE), and relative bias (RB). The CC evaluates the linear agreement between the datasets, whereas RMSE and MAE quantify the magnitude of the estimation error. The equations are defined as follows:

$$CC = \frac{\sum_{i=1}^{n}(O_i - \bar{O})(E_i - \bar{E})}{\sqrt{\sum_{i=1}^{n}(O_i - \bar{O})^2}\sqrt{\sum_{i=1}^{n}(E_i - \bar{E})^2}} \quad (1)$$

$$RMSE = \sqrt{\frac{1}{n}\sum_{i=1}^{n}(E_i - O_i)^2} \quad (2)$$

$$MAE = \frac{1}{n}\sum_{i=1}^{n}|E_i - O_i| \quad (3)$$

$$RB(\%) = \frac{\sum_{i=1}^{n}(S_i - O_i)}{\sum_{i=1}^{n} O_i} \times 100 \quad (4)$$

where E_i and O_i denote the satellite-estimated and gauge-observed precipitation for day i, respectively, and n is the total number of days.
To address rigorous hydrological evaluation standards, the Nash–Sutcliffe efficiency (NSE) and Kling–Gupta efficiency (KGE) were incorporated. NSE normalizes the model's error variance against the observed variance, while KGE provides a diagnostically robust metric by simultaneously evaluating correlation, spatial variability bias, and mean bias. These are calculated as:

$$NSE = 1 - \frac{\sum_{i=1}^{n}(E_i - O_i)^2}{\sum_{i=1}^{n}(O_i - \bar{O})^2} \quad (5)$$

$$KGE = 1 - \sqrt{(r-1)^2 + (\alpha - 1)^2 + (\beta - 1)^2} \quad (6)$$

where r is the Pearson correlation coefficient between estimates and observations (equivalent to CC), $\alpha = \sigma_E/\sigma_O$ represents the ratio of the standard deviation of the estimated values (σ_E) to that of the observed values (σ_O), and $\beta = \bar{E}/\bar{O}$ is the ratio of their respective means.

2.3. Categorical evaluation (precipitation detection)

To assess the capability of the satellite products in accurately detecting precipitation events (rain/no-rain discrimination), categorical metrics were calculated using a daily precipitation threshold of 0.1 mm. This threshold was selected because 0.1 mm represents the minimum measurable amount of precipitation by standard ground-based rain gauges. Furthermore, adopting this threshold effectively filters out non-precipitating clouds, light dew, and instrumental noise, thereby preventing artificial inflation of the false alarm ratio (FAR) and ensuring a reliable calculation of categorical metrics (Tang *et al.* 2020; Tian *et al.* 2018). The metrics include the Probability of Detection (POD), FAR, and Critical Success Index (CSI).

$$POD = \frac{H}{H + M} \quad (7)$$

$$FAR = \frac{F}{H + F} \quad (8)$$

$$CSI = \frac{H}{H + M + F} \quad (9)$$

where, H (Hits) represents events correctly detected by the satellite, M (Misses) denotes observed events missed by the satellite, and F (false alarms) indicates events erroneously reported by the satellite when no rain was observed.

2.3. Bias correction using MLR

To mitigate the systematic errors inherent in satellite retrievals, a MLR model was developed. Unlike conventional linear scaling that only utilizes precipitation data, this study incorporates local meteorological covariates to dynamically adjust the satellite estimates. The MLR model is expressed as:

$$P_{corrected} = \beta_0 + \beta_1 P_{sat} + \beta_2 T_{max} + \beta_3 RH + \beta_4 WS \quad (10)$$

where, $P_{corrected}$ is the adjusted daily precipitation, P_{sat} is the raw satellite estimate (IMERG or GSMaP), and β_0 to β_4 are the regression coefficients optimized using the ordinary least squares method. To ensure the statistical validity of the MLR model, fundamental regression assumptions were rigorously tested prior to modeling. Multicollinearity among the predictors was assessed using the variance inflation factor (VIF), confirming that all values remained well below the critical threshold of 5. Furthermore, to prevent overfitting and guarantee model robustness, a rigorous k-fold cross-validation (k=5) approach was implemented across the 18-year dataset, replacing the conventional data-split method. Negative corrected precipitation values, which lack physical meaning, were subsequently forced to zero.

3. Results and discussion

3.1. Baseline evaluation of gridded precipitation products

To attain a precise understanding of the systematic and random errors associated with the precipitation products, the initial step evaluated the daily-scale performance of the IMERG and GSMaP satellites against observational data from the Birjand synoptic station. The continuous statistical metrics (Table 1) reveal significant differences in the accuracy of these two products. GSMaP demonstrated considerable superiority over IMERG, recording a CC of 0.677 and a RMSE of 3.25 mm/day, compared to IMERG's CC of 0.416 and RMSE of 4.40 mm/day. The slightly better performance of GSMaP in certain arid and semi-arid topographies aligns with recent regional evaluations (Tosan *et al.* 2026c). The superior performance of GSMaP in this hyper-arid environment can be attributed to its specialized Orographic/Topographic Rainfall effect correction and the specific parameterization of its passive microwave (PMW) retrieval algorithm. These algorithmic adjustments appear more adept at filtering out false precipitation signals associated with sub-cloud evaporation over hot and dry land surfaces compared to IMERG.

Table 1. Continuous statistical metrics for the performance evaluation of satellite precipitation products.

Satellite product	CC (Pearson)	RMSE (mm/day)	MAE (mm/day)	RB (%)
IMERG (Final V07)	0.416	4.40	2.49	-7.5
GSMaP	0.677	3.25	1.70	-15.5

The scatter plots (Fig. 2a and 2b) further confirm that GSMaP estimates are more consistent with the reference line (1:1), whereas the dispersion of IMERG data increases notably, particularly during heavier rainfall events. A critical point in Table 1 is the presence of a negative RB in both products (-7.5% for IMERG and -15.5% for GSMaP). This systematic underestimation in arid regions is largely attributed to the sub-cloud evaporation of raindrops before reaching the surface—known as the Virga effect (Nikoo *et al.* 2026)—as well as the combined effects of wind and topography leading to inaccurate retrievals by passive microwave sensors (Tan *et al.* 2026). Despite this, the monthly precipitation distribution (Fig. 2c) demonstrates that both products successfully simulated the region's seasonal precipitation regime, including the winter and spring peaks, with acceptable accuracy.

3.2. Categorical evaluation (precipitation detection)

Beyond quantitative values, the ability of the gridded products to correctly detect the occurrence or non-occurrence of precipitation (using a 0.1 mm threshold) was assessed using categorical indices (Fig. 3). The results indicate a contrasting and noteworthy behavior between the two products. IMERG exhibited very high sensitivity in tracking precipitation systems, recording a POD of 0.763, meaning it correctly identified over 76% of rainy days at the Birjand station. However, as observed in similar continental evaluations, this high sensitivity leads to an overestimation of precipitation frequency, increasing the FAR to 0.340 (Xiong *et al.* 2025).

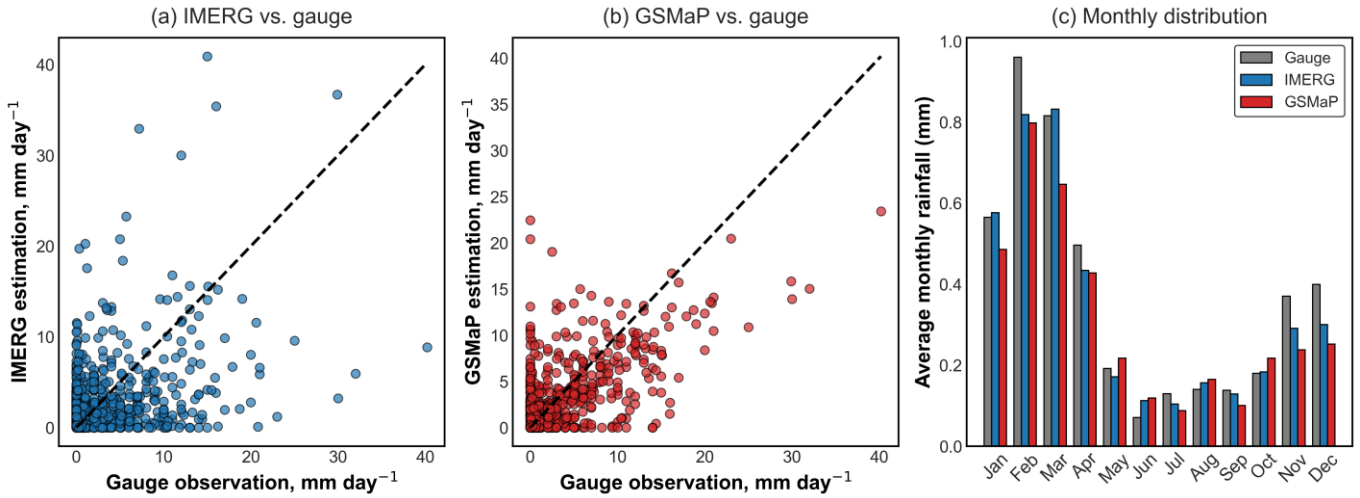

Fig. 2. Baseline performance of satellite products: (a) Scatter plot of IMERG vs. gauge observations; (b) Scatter plot of GSMaP vs. gauge observations, with the dashed black line representing the 1:1 reference line; and (c) Comparison of average monthly precipitation distribution over the 18-year period.

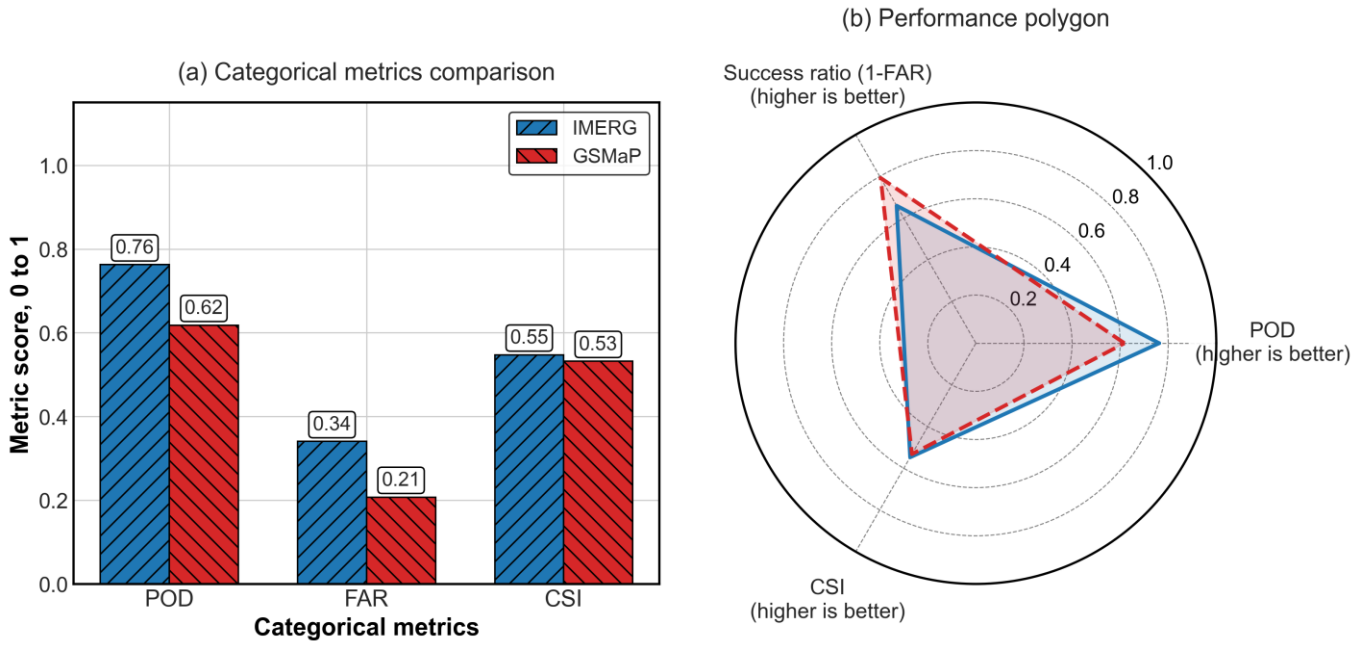

Fig. 3. Bar chart comparing (a) categorical metrics, POD, FAR, and (b) CSI, for IMERG and GSMaP, using a 0.1 mm/day precipitation threshold.

In contrast, GSMaP adopted a more conservative approach. Although its detection strength (POD = 0.618) was lower than that of IMERG, its stricter algorithms resulted in a significantly lower false alarm (FAR = 0.207). Ultimately, the CSI, which represents the overall performance of the model in detecting precipitation, showed that both products achieved similar final performance in distinguishing wet and dry days in the region's climate (CSI ≈ 0.53 to 0.54). This contrast, IMERG's high sensitivity versus GSMaP's high precision, serves as a vital guide for selecting datasets in drought monitoring and early warning systems (Gheysouri *et al.* 2025).

3.3. Sensitivity analysis of satellite errors to thermodynamic and dynamic atmospheric conditions

To better comprehend the physical mechanisms affecting the uncertainty of precipitation products, the relationship between the absolute errors of IMERG and GSMaP estimates and the meteorological parameters of the Birjand station (maximum temperature, relative humidity, and wind speed) was evaluated using 2D density distribution plots (Fig. 4) and the Pearson correlation test. The statistical analysis revealed a significant relationship (at a 99% confidence level, P-value < 0.01) between satellite errors and thermodynamic variables. Quantitatively, as illustrated in the correlation heatmap (Figure 5), maximum temperature exhibits a significant negative correlation with estimation error (r = -0.103 for IMERG and r = -0.120 for GSMaP). The concentration of error density at lower temperatures in the bivariate KDE plots (Figure 4) physically corroborates that satellite sensors experience reduced accuracy during cold seasons when encountering cold cloud systems and solid precipitation. This thermodynamic limitation aligns perfectly with recent global benchmark studies (e.g., Sohi *et al.* 2025; Xiong *et al.* 2025), which highlighted the inherent uncertainties of PMW retrievals over cold surfaces. On the other hand, relative humidity exhibited a significant positive correlation (r ≈ 0.20) with the absolute error magnitude. This confirms that in hyper-arid environments, dry sub-cloud layers aggressively evaporate falling precipitation (the Virga effect), causing the satellites to drastically overestimate surface rainfall, a critical hydrological implication for flash flood early warning systems in desert basins (Nikoo *et al.* 2026).

On the other hand, relative humidity exhibited a significant positive correlation (r ≈ 0.20) with the absolute error magnitude. Conversely, examining the effect of the dynamic parameter (wind speed) on the error margin showed no statistically significant relationship (P-value > 0.05) between wind speed and the error of gridded products in the study area, contradicting common assumptions about wind-induced undercatch. This finding proves that in the arid climate of South Khorasan, satellite errors are primarily thermodynamic in nature rather than dynamic. Details of the Pearson correlations among all hydro-climatic variables are visually summarized in the correlation heatmap (Fig. 5).

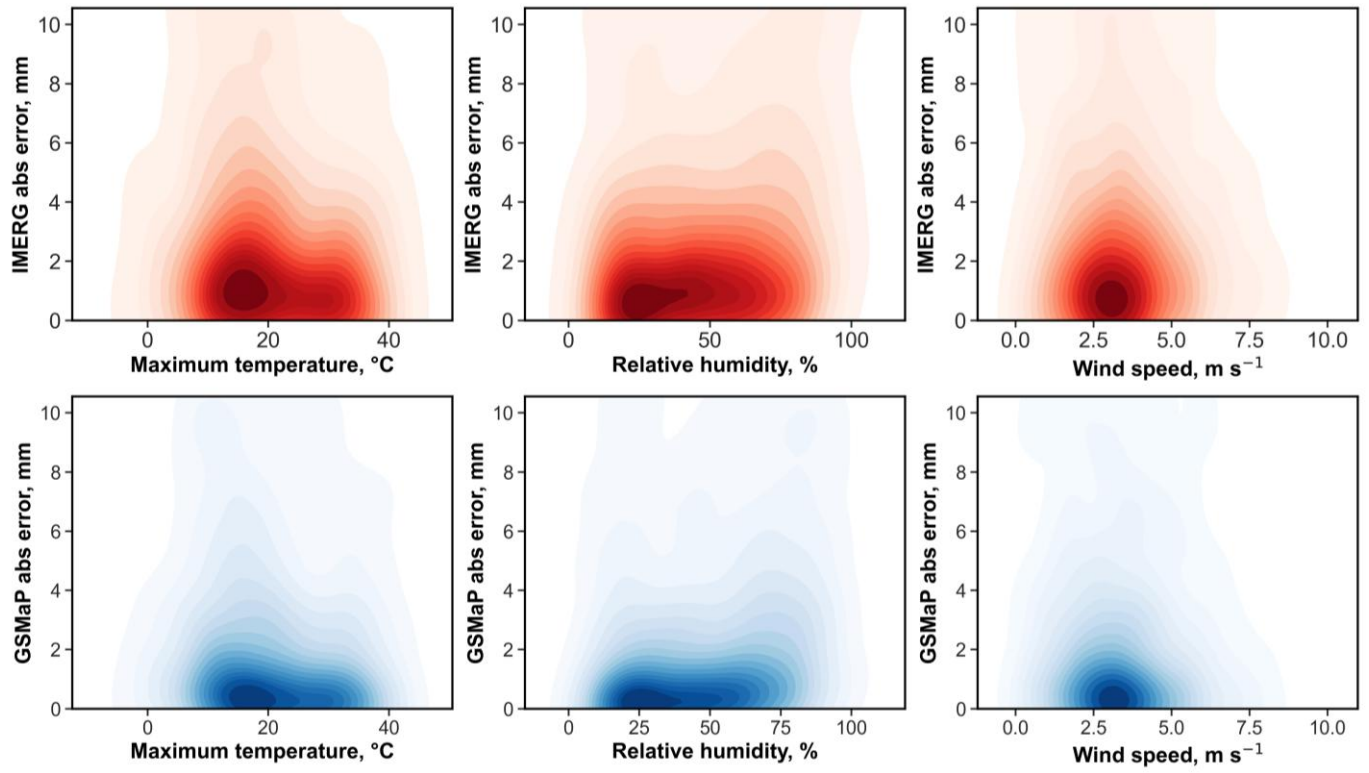

Fig. 4. Bivariate density distribution (KDE) plots illustrating the concentration of satellite absolute estimation errors under varying surface meteorological conditions: maximum temperature (left), relative humidity (middle), and wind speed (right).

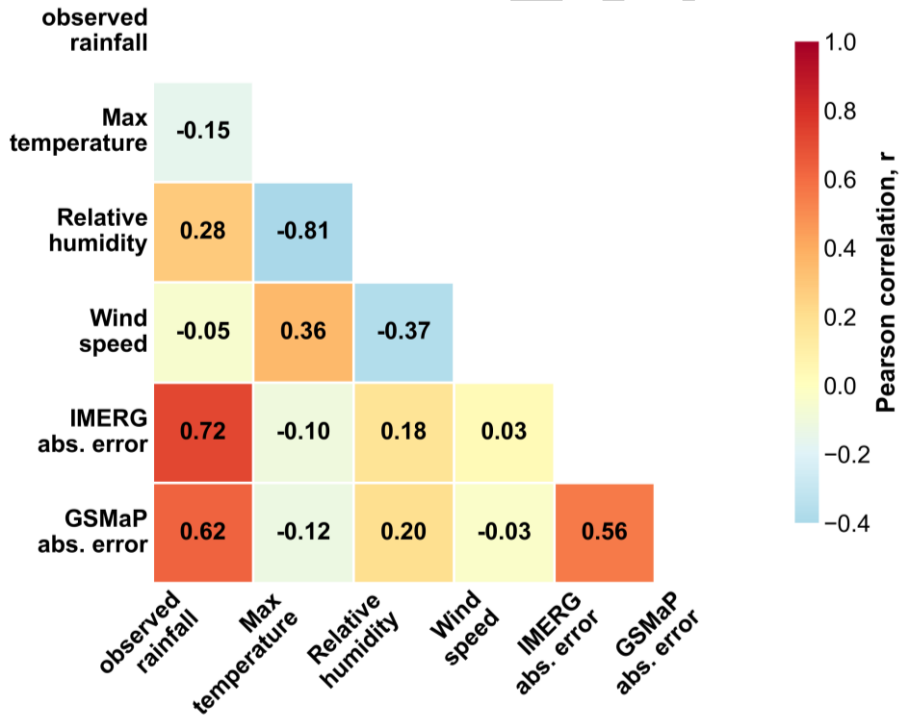

Fig. 5. Pearson correlation matrix (Heatmap) of hydro-climatic variables and satellite absolute errors.

3.4. Precipitation estimation improvement using MLR

Having established the sensitivity of satellite product errors to meteorological variables, the final step evaluated the efficacy of a MLR model to correct satellite estimates. In this framework, the initial satellite estimate, along with maximum temperature, relative humidity, and wind speed, were inputted as predictors, while the synoptic station precipitation served as the target variable. The integration of meteorological covariates into machine learning and regression frameworks has recently been proven to significantly enhance bias correction performance (Yao *et al.* 2024). The model evaluation results (Table 2 and Fig. 6) demonstrate the effectiveness of this approach, particularly for IMERG. Applying the meteorological correction to IMERG data reduced the RMSE from 4.40 to 3.78 mm/day, representing a measurable 14.1% improvement. Simultaneously, the CC for this product improved from 0.416 to 0.493.

Table 2. Performance evaluation of the MLR model in correcting the errors of satellite precipitation products.

Product / state	CC	RMSE (mm/day)	MAE (mm/day)	NSE	KGE
IMERG (original)	0.416	4.40	2.49	-0.027	0.395
IMERG (corrected)	0.493	3.78	2.34	0.243	0.278

The scatter plots (Fig. 6a and 6b) clearly illustrate that after applying the model, the dispersion of erroneous data decreased, and

the corrected values converged much better toward the ideal 1:1 line. Similar bias correction techniques, such as Artificial Neural Networks (ANN), have also shown substantial RMSE reduction in neighboring arid regions like Saudi Arabia (Elsebaie *et al.* 2025).

In contrast, GSMaP, which already possessed high baseline accuracy in the region, experienced a more conservative improvement (a 4.4% reduction in RMSE and a CC increase to 0.699). This significant difference in responsiveness to the correction model proves that IMERG's retrieval algorithms suffer from greater weaknesses in understanding local thermodynamic conditions in the arid regions of the Middle East. Integrating these algorithms with surface temperature and humidity data can largely compensate for this algorithmic limitation (Zhang *et al.* 2025b). The findings of this section offer a lightweight, practical, and reliable computational framework for water resource engineers to generate more accurate precipitation data in poorly gauged basins. To further validate the robustness of the MLR model, advanced hydrological metrics were evaluated. The application of the correction framework remarkably improved the NSE for IMERG from a negative value (-0.027) to a positive skill score (0.243), indicating that he corrected estimates transitioned from being worse than the observed mean to possessing actual predictive skill. Conversely, the KGE experienced a slight decrease from 0.395 to 0.278. This behavior is a well-documented mathematical characteristic of linear regression models; while MLR effectively minimizes absolute errors (hence improving RMSE and NSE), it inherently compresses the variance of the predicted values, which adversely affects the variability ratio (α) component of the KGE metric. Furthermore, a 5-fold cross-validation confirmed the model's temporal stability, yielding a consistent mean R2 of 0.224 across folds without signs of overfitting.

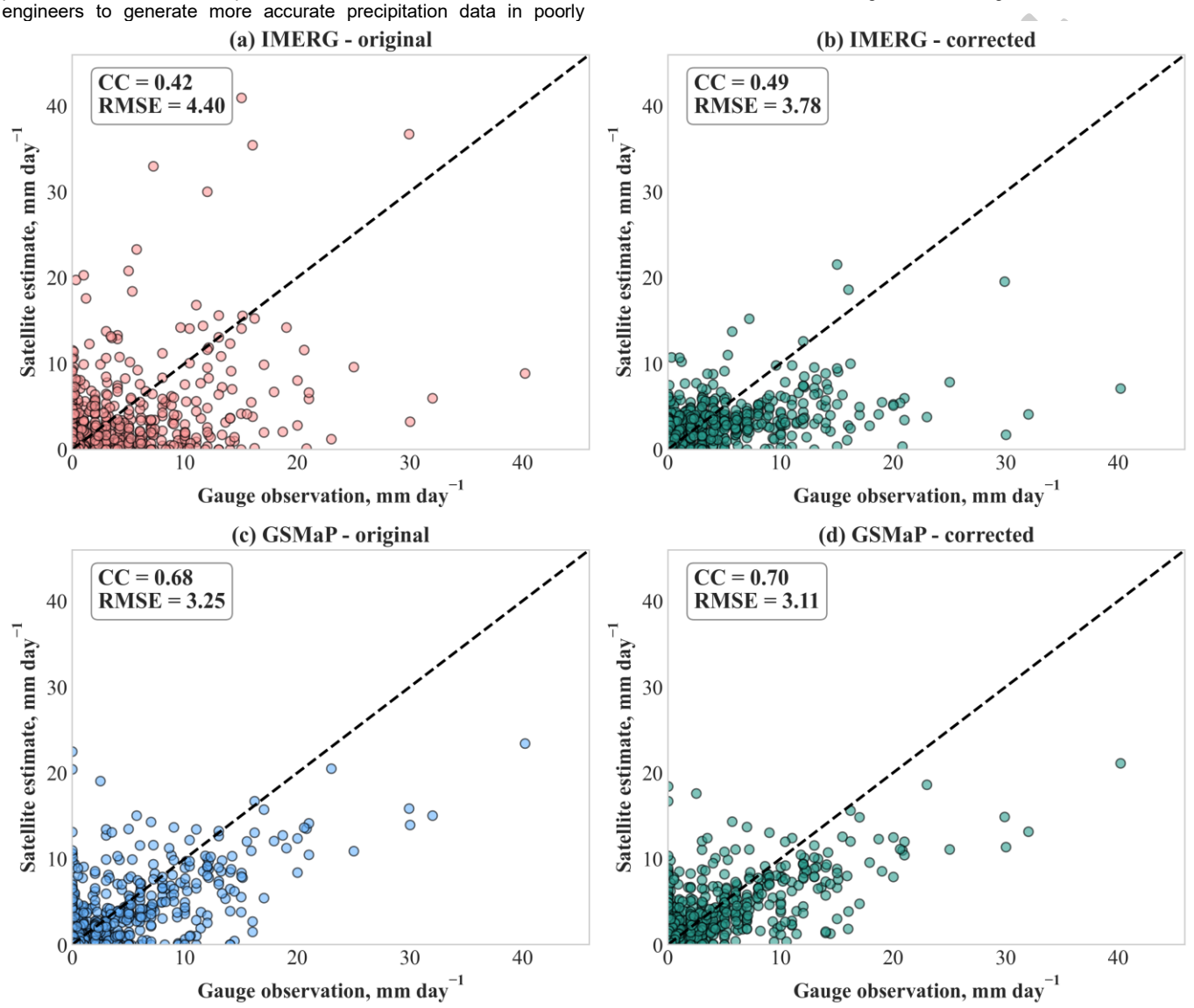

Figure 6. Scatter plots comparing original and MLR-corrected satellite precipitation estimates against gauge observations.

4. Conclusions

This study comprehensively evaluated the performance of two leading satellite precipitation products, IMERG (Final Run V07) and GSMaP, against 18 years (2005–2023) of daily synoptic observations in eastern Iran. Subsequently, it investigated the meteorological drivers of estimation uncertainties and proposed a bias correction framework using MLR. The baseline evaluation revealed that GSMaP generally outperformed IMERG in continuous statistical metrics (RMSE = 3.25 vs. 4.40 mm/day). However, both products exhibited a systematic underestimation (negative RB), primarily driven by the sub-cloud evaporation of raindrops (the Virga effect) which is highly prevalent in arid climates. From a categorical perspective, IMERG demonstrated a higher sensitivity and POD = 0.763 at the cost of elevated false alarms, whereas GSMaP provided a more conservative but precise detection capability. An important finding of this research is the pronounced sensitivity of satellite retrieval errors to local thermodynamic conditions. Bivariate density analysis and correlation tests confirmed that absolute estimation errors significantly increase under lower temperatures and higher relative humidity (P-value < 0.01). This indicates the ongoing limitations of microwave sensors in detecting solid precipitation and cold cloud systems. Conversely, the dynamic effect of wind speed showed no statistically significant impact on precipitation estimation errors, demonstrating that satellite uncertainties in this specific hyper-arid environment are primarily thermodynamic rather than dynamic. Addressing these thermodynamic uncertainties, the integration of surface meteorological covariates (maximum temperature, relative humidity, and wind speed) into an MLR bias correction model yielded substantial improvements. The proposed framework successfully reduced the RMSE of IMERG by 14.1% and increased its CC, effectively mitigating the inherent retrieval biases and pulling the scattered estimates closer to the 1:1 reference line. It is important to

acknowledge that this study relies on long-term observations from a single synoptic station, which may limit the spatial representation of the findings. While Birjand serves as an excellent representative of hyper-arid conditions, further investigations incorporating a denser network of gauges across diverse topographies are recommended to confirm the spatial generalizability of these thermodynamic relationships across other hyper-arid basins. Ultimately, this study demonstrates that while raw SPPs possess inherent uncertainties in hyper-arid regions, their integration with local meteorological variables through lightweight machine learning and regression algorithms can generate significantly improved datasets. These corrected, high-resolution precipitation products hold significant potential for advancing hydrological modeling, extreme event forecasting, and sustainable water resource management in data-scarce environments.

Author Contributions

Mahdi Naseri: Conceptualization, Methodology, Formal analysis, Investigation, Writing original draft, Writing review & editing, Visualization, Project administration.
Mitra Noorizehab: Data curation, Validation, Investigation, Software, Writing review & editing, Resources, Formal analysis, Data curation.

Conflict of Interest

The authors declare that they have no competing interests

Data Availability Statement

The data that support the findings of this study are fully presented within this article and have not been previously published elsewhere.

References

Akbarpour, A. *et al.* (2024) 'Performance analysis of finite element method in groundwater studies based on Web of Science using R Biblioshiny', *Journal of Aquifer and Qanat*, 4(2), pp. 131-148. doi: https://doi.org/10.22077/jaaq.2024.7481.1071

Baig, F. *et al.* (2025) 'From bias to accuracy: Transforming satellite precipitation data in arid regions with machine learning and topographical insights', *Journal of Hydrology*, 653, p. 132801. doi: https://doi.org/10.1016/j.jhydrol.2025.132801

Bisht, D. S. *et al.* (2025) 'Bias correction of satellite precipitation estimates using Mumbai-MESONET observations: A Random Forest approach', *Atmospheric Research*, 315, p. 107858. doi: https://doi.org/10.1016/j.atmosres.2024.107858

Cao, C. *et al.* (2025) 'Regionalization of hydrological cycle changes in 31 source catchments of Yellow River Basin considering multiple hydrological variables', *Journal of Hydrology: Regional Studies*, 59, p. 102340. doi: https://doi.org/10.1016/j.ejrh.2025.102340

Conte, L. C., Tassi, R., and Bayer, D. M. (2026) 'Satellite-based rainfall datasets: A global systematic review of applications, accuracy, and research gaps', *IEEE Access*, 14, pp. 29539-29565. doi: https://doi.org/10.1109/ACCESS.2026.3667060

Elsebaie, I. H. *et al.* (2025) 'Bias correction methods applied to satellite rainfall products over the western part of Saudi Arabia', Atmosphere, 16(7), p. 772. doi: https://doi.org/10.3390/atmos16070772

Feizi, H. and Tosan, M. (2017) 'Saffron yield variability by climatic factors in the northeast of Iran', Saffron Agronomy and Technology, 5(1), pp. 3-17. doi: https://doi.org/10.22048/JSAT.2017.43324

Gheysouri, M. *et al.* (2025) 'Evaluation of IMERG precipitation product in the investigation of drought events in the Kermanshah Province', Acta Geophysica, 73, pp. 2669-2682. doi: https://doi.org/10.1007/s11600-025-01558-w

Gou, J. *et al.* (2026) 'Uncertainty quantification of satellite-based essential climate variables derived from deep learning', *Surveys in Geophysics*, In Press. doi: https://doi.org/10.1007/s10712-025-09919-2

Ji, W. *et al.* (2025) 'An integrating pre-temperature description method for generating all-weather land surface temperature via passive microwave and thermal infrared remote sensing', *Remote Sensing of Environment*, 324, p. 114767. doi: https://doi.org/10.1016/j.rse.2025.114767

Li, W. *et al.* (2025) 'Groundwater recharge estimation in data-limited water-scarce regions', *Hydrology Research*, 56(6), pp. 439-458. doi: https://doi.org/10.2166/nh.2025.122

Mardani, M. *et al.* (2025) 'A bibliometric analysis of research trends on the application of remote sensing in precipitation estimation with an emphasis on spatio-temporal analysis in Iran', *Iranian Journal of Rainwater Catchment Systems*, 13(2), pp. 101-118. dor: https://dor.org/20.1001.1.24235970.1404.13.2.1.3

Meng, H. and Zhao, T. (2025) 'Evaluation of the hydrological utility of the GPM IMERG satellite precipitation products', *Atmospheric Research*, 322, p. 108139. doi: https://doi.org/10.1016/j.atmosres.2025.108139

Montiel, J. I. P., Epiayu, A. M. C., and Moscote, C. D. (2026) 'Evaluation of Satellite Precipitation Products across Climatic and Topographic Gradients in a Basin in Northern South America', *Environmental Challenges*, 22, p. 101426. doi: https://doi.org/10.1016/j.envc.2026.101426

Nikoo, M. R. *et al.* (2026) 'Assessing the fidelity of multi-satellite precipitation estimates for drought monitoring in a mountain water tower to arid basin system', *Journal of Arid Environments*, 232, p. 105519. doi: https://doi.org/10.1016/j.jaridenv.2025.105519

Nourani, V. *et al.* (2025) 'Advances in multi-source data fusion for precipitation estimation: remote sensing and machine learning perspectives', *Earth-Science Reviews*, 270, p. 105253. doi: https://doi.org/10.1016/j.earscirev.2025.105253

Pellicone, G. *et al.* (2025) 'Assessment of multiple satellite precipitation products over Italy', *Remote Sensing*, 17(22), p. 3772. doi: https://doi.org/10.3390/rs17223772

Ramezani Moghadam, J., Yaghoubzadeh, M., and Jafarzadeh, A. (2018) 'Examination of feature selection methods for downscaling of daily precipitation in two different climates', *Water and Soil*, 32(4), pp. 831-848. doi: https://doi.org/10.22067/jsw.v32i4.72732

Rezvani Moghaddam, P. *et al.* (2016) 'Saffron agronomy and technology (book of abstracts: 2013-2016)', *Saffron Agronomy and Technology*, 4, pp. 1-78. doi: https://doi.org/10.22048/jsat.2016.39250

Saeed Abdelrazaq, A. *et al.* (2026) 'Benchmarking MSWEP precipitation accuracy in arid zones against traditional and satellite measurements', *Remote Sensing*, 18(1), p. 95. doi: https://doi.org/10.3390/rs18010095

Shamshirgaran, R., Tosan, M., and Nasirian, A. (2025) 'Investigating the functional problems of ground water studies in dry areas: a case of Boshruyeh Plain, South Khorasan, Iran', *Journal of Aquifer and Qanat*, 5(2), pp. 99-120. doi: https://doi.org/10.22077/jaaq.2025.8734.1094

Shirmohammadi Aliakbarkhani, Z. *et al.* (2025) 'Assessing the Standardized Precipitation Index Utilizing Satellite-Based and Reanalyzed Precipitation Products in Semi-Arid Region, Iran', *Journal of the Indian Society of Remote Sensing*, 53(10), pp. 3393-3407. doi: https://doi.org/10.1007/s12524-025-02152-9

Sohi, H. Y., Farmani, M. A., and Behrangi, A. (2025) 'How do IMERG V07, IMERG V06, and ERA5 precipitation products perform over snow–ice-free and snow–ice-covered surfaces at a range of near-surface temperatures?', *Journal of Hydrometeorology*, 26(7), pp. 837-855. doi: https://doi.org/10.1175/JHM-D-24-0110.1

Tan, A. *et al.* (2026) 'Comparative assessment of eight satellite precipitation products over the complex terrain of the lower Yarlung Zangpo basin: Performance evaluation and topographic influence analysis', *Remote Sensing*, 18(1), p. 63. doi: https://doi.org/10.3390/rs18010063

Tang, G. *et al.* (2020) 'Have satellite precipitation products improved over last two decades? A comprehensive comparison of GPM IMERG with nine satellite and reanalysis datasets', *Remote Sensing of Environment*, 240, p. 111697. doi: https://doi.org/10.1016/j.rse.2020.111697

Tian, F. *et al.* (2018) 'How does the evaluation of the GPM IMERG precipitation product depend on gauge density and rainfall intensity? ', *Journal of Hydrometeorology*, 19(2), pp. 339-349. doi: https://doi.org/10.1175/JHM-D-17-0161.1

Tosan, M. *et al.* (2024) 'A review of smart water management for sustainable agriculture based on the internet of things', *Water Management in Agriculture*, 11(1), pp. 145-166. Available at:

https://wmaj.iaid.ir/article_185939.html?lang=en (Accessed date: 21 April 2025).

Tosan, M. and Maroosi, A. (2024) 'Investigating the performance of artificial rabbit optimization hybrid algorithm (ANN-ARO) in forecasting reference evapotranspiration with limited climatic parameters', *Iranian Journal of Rainwater Catchment Systems*, 12(1), pp. 47-66. dor: https://dor.isc.ac/dor/20.1001.1.24235970.1403.12.1.3.6

Tosan, M. *et al.* (2026a) 'The transparency revolution in geohazard science: a systematic review and research roadmap for explainable artificial intelligence', *Computer Modeling in Engineering & Sciences*, 146(1), p. 3. doi: https://doi.org/10.32604/cmes.2025.074768

Tosan, M., Nourani, V., and Uzelaltinbulat, S. (2026b) 'Linking the skill of multi-satellite precipitation estimates to the synoptic drivers of extreme events across a mountain-desert transition zone', *Theoretical and Applied Climatology*, 157, p. 376. doi: https://doi.org/10.1007/s00704-026-06312-w

Tosan, M. *et al.* (2026c) 'Spatiotemporal performance and error analysis of satellite precipitation products over a topographically complex semi-arid region in Iran', *Journal of Mountain Science*, 23, pp. 118-138. doi: https://doi.org/10.1007/s11629-025-9984-6

Xiong, J., Tang, G., and Yang, Y. (2025) 'Continental evaluation of GPM IMERG V07B precipitation on a sub-daily scale', *Remote Sensing of Environment*, 321, p. 114690. doi: https://doi.org/10.1016/j.rse.2025.114690

Yao, N. *et al.* (2024) 'Bias correction of the hourly satellite precipitation product using machine learning methods enhanced with high-resolution WRF meteorological simulations', *Atmospheric Research*, 310, p. 107637. doi: https://doi.org/10.1016/j.atmosres.2024.107637

Yaqubi, M., Yaghoobzadeh, M., and Tosan, M. (2024) 'Factor analysis and ranking of saffron production, processing and market challenges in Torbat Heydarieh, Iran', *Saffron Agronomy and Technology*, 12(1), pp. 81-111. doi: https://doi.org/10.22048/jsat.2024.436229.1518

Zhang, L. *et al.* (2025a) 'Evaluation and statistical bias correction of ERA5-Land meteorological variables for a humid river basin in Southwest China', *Scientific Reports*, 15, p. 41101. doi: https://doi.org/10.1038/s41598-025-24942-4

Zhang, Q. *et al.* (2025b) 'Swat+ model enhanced with dynamic phenology remote sensing and high-precision precipitation data for water resource vulnerability assessment in semi-arid regions', *Water Resources Management*, 39(10), pp. 4947-4969. doi: https://doi.org/10.1007/s11269-025-04182-